Effects of electron irradiation on resistivity and London penetration depth of $Ba_{1-x}K_xFe_2As_2$ ($x \leqslant 0.34$) iron-pnictide superconductor

K. Cho,[1] M. Kończykowski,[2] J. Murphy,[1] H. Kim,[1] M. A. Tanatar,[1] W. E. Straszheim,[1] B. Shen,[3] H. H. Wen,[3] and R. Prozorov[1,*]

[1]*Ames Laboratory and Department of Physics and Astronomy, Iowa State University, Ames, Iowa 50011, USA*

[2]*Laboratoire des Solides Irradiés, CNRS UMR 7642 and CEA-DSM-IRAMIS, Ecole Polytechnique, F-91128 Palaiseau Cedex, France*

[3]*Center for Superconducting Physics and Materials, National Laboratory of Solid State Microstructures and Department of Physics, Nanjing University, Nanjing 210093, China*

(Received 28 July 2014; revised manuscript received 4 September 2014; published 19 September 2014)

Irradiation with 2.5 MeV electrons at doses up to 5.2×10^{19} electrons/cm^2 was used to introduce pointlike defects in single crystals of $Ba_{1-x}K_xFe_2As_2$ with $x = 0.19$ ($T_c = 14$ K), 0.26 ($T_c = 32$ K), 0.32 ($T_c = 37$ K), and 0.34 ($T_c = 39$ K) to study the superconducting gap structure by probing the effect of nonmagnetic scattering on electrical resistivity $\rho(T)$ and London penetration depth $\lambda(T)$. For all compositions, the irradiation suppressed the superconducting transition temperature T_c and increased resistivity. The low-temperature behavior of $\lambda(T)$ is best described by the power-law function, $\Delta\lambda(T) = A(T/T_c)^n$. While substantial suppression of T_c supports $s_\pm$ pairing, in samples close to the optimal doping, $x = 0.26$, 0.32, and 0.34, the exponent n remained high ($n \geqslant 3$), indicating almost exponential attenuation and thus a robust full superconducting gap. For the $x = 0.19$ composition, which exhibits coexistence of superconductivity and long-range magnetism, the suppression of T_c was much more rapid, and the exponent n decreased toward the $s_\pm$ dirty limit of $n = 2$. In this sample, the irradiation also suppressed the temperature of structural/magnetic transition T_{sm} from 103 to 98 K, consistent with the itinerant nature of the long-range magnetic order. Our results suggest that underdoped compositions, especially in the coexisting regime, are most susceptible to nonmagnetic scattering and imply that in multiband $Ba_{1-x}K_xFe_2As_2$ superconductors, the ratio of the interband to intraband pairing strength, as well as the related gap anisotropy, increases upon the departure from the optimal doping.

DOI: 10.1103/PhysRevB.90.104514 PACS number(s): 74.70.Xa, 74.20.Rp, 74.62.Dh

I. INTRODUCTION

Studying the effects of controlled pointlike disorder on superconducting properties is a powerful tool to understand the mechanism of superconductivity [1–8]. According to Anderson's theorem, conventional isotropic s-wave superconductors are not affected by the potential (nonmagnetic) scattering but are sensitive to spin-flip scattering on magnetic impurities [1]. In high-T_c cuprates, both magnetic and nonmagnetic impurities cause rapid suppression of the superconducting transition temperature T_c, strongly supporting d-wave pairing [9]. Similarly, for an order parameter changing sign between the sheets of the Fermi surface ($s_\pm$ pairing), considered most plausible in multiband iron-based superconductors (FeSCs) [10–12], the response to nonmagnetic scattering is expected to be significant [12,13]. We should note that the multiband character of superconductivity itself does not lead to the anomalous response to nonmagnetic disorder beyond expected smearing of the gap variation on the Fermi surface, including the difference in gap magnitudes between the different bands [14]. For example, in a known two-gap s_{++} superconductor, MgB_2, electron irradiation resulted only in a minor change in T_c [15]. The sign change of the order parameter either along one sheet of the Fermi surface or between the sheets is what causes the dramatic suppression of T_c due to the pair-breaking nature of interband scattering in this case.

A relatively slow rate of T_c suppression with disorder found in several experiments in iron-based superconductors was used as an argument for the s_{++} pairing, expected for superconductivity mediated by orbital fluctuations [16,17]. In reality, the situation in sign-changing multiband superconductors is more complicated due to the competition between intraband and interband pairing and also band-dependent scattering times and gap anisotropies [6,11,12]. Realistic calculations of the effect of pointlike disorder on T_c within the $s_\pm$ scenario [6] agree very well with the experiment, for example, in electron-irradiated $Ba(Fe_{1-x}Ru_x)_2As_2$ [7] and $BaFe_2(As_{1-x}P_x)_2$ [8].

Experimentally, it is quite difficult to introduce controlled pointlike disorder. The superconducting and normal state properties changed in significantly different way when disorder was introduced either by chemical substitution [18–20] or by heavy ion or particle irradiation [21–26]. Chemical substitution changes both the crystalline and electronic structures, and most particle irradiations introduce correlated disorder in the form of columnar defects and/or clusters of different spatial extent [27]. The effective scattering potential strength and range (size) of such defects are very different from pointlike scattering. On the other hand, MeV-range electron irradiation is known to produce vacancy-interstitial (Frenkel) pairs, which act as efficient pointlike scattering centers [27]. This is consistent with the analysis of the collective pinning in $BaFe_2(As_{1-x}P_x)_2$ and $Ba(Fe_{1-x}Co_x)_2As_2$ [28] as well as the penetration depth in $BaFe_2(As_{1-x}P_x)_2$ [8]. In the high-T_c cuprates, electron-irradiation defects are known to be

*Corresponding author: prozorov@ameslab.gov

strong unitary scatterers that cause significant suppression of T_c [29].

In addition to T_c, another parameter sensitive to disorder is quasiparticle density, which may be probed, for example, by measuring the London penetration depth $\lambda(T)$. In the case of isotropic single-band s-wave or multiband s_{++}-wave superconductors, $\lambda(T)$ remains exponential at low temperatures with the addition of nonmagnetic scattering [6,13,30], whereas in the case of nodeless $s_{\pm}$ pairing it changes from exponential in the clean limit to $\sim T^2$ in the dirty limit [6,13]. However, an opposite behavior is observed in superconductors with line nodes where $\lambda \sim T$ in the clean limit changes to $\sim T^2$ in the dirty limit [3,31–33]. In the case of pnictide superconductors with accidental nodes, $\lambda(T)$ evolves from linear to exponential and, ultimately, to the T^2 behavior [8]. The details of the evolution from the clean to dirty limit also depend on the (usually unknown) scattering potential amplitude and spatial extent. A weak Born scattering approximation, usually valid for normal metals, could not explain the rapid $T \rightarrow T^2$ evolution in the cuprates, so the unitary limit was used instead [4,33]. In iron-based superconductors, the situation is unclear, and it seems that intermediate scattering amplitudes (modeled within the T-matrix approach) are needed [6,7,13]. The spatial extent of the scattering potential affects the predominant scattering Q vector, and it was suggested as the cause of a notable difference in quasiparticle response and evolution of T_c in $SrFe_2(As_{1-x}P_x)_2$ with natural and artificial disorders [34].

In this paper, we study the effects of electron irradiation on superconducting T_c and quasiparticle excitations of hole-doped $(Ba_{1-x}K_x)Fe_2As_2$ single crystals by measuring in-plane resistivity $\rho(T)$ and in-plane London penetration depth $\Delta\lambda(T)$. $(Ba_{1-x}K_x)Fe_2As_2$ has the highest $T_c \approx 40$ K within the 122 family and at the optimal doping reveals extremely robust superconductivity [25,35,36]. The superconducting gap structure of $(Ba_{1-x}K_x)Fe_2As_2$ varies with the composition from a full isotropic gap at the optimal doping to a gap with line nodes at $x = 1$ [37–39]. On the underdoped side of interest here, gap anisotropy increases toward the edge of the superconducting dome, especially in the range of bulk coexistence of superconductivity and long-range magnetic order [36,40]. This might imply that the ratio of the interband to intraband pairing, as well as gap anisotropy, increases upon the departure from the optimal doping.

II. EXPERIMENT

Single crystals of $(Ba_{1-x}K_x)Fe_2As_2$ were synthesized using the high-temperature FeAs flux method [42]. The samples used in this study were cleaved from the inner parts of single crystals and were first extensively characterized using rf magnetic susceptibility as well as magneto-optical imaging to exclude chemical and spatial inhomogeneity. The compositions of $x = 0.19$, 0.26, and 0.34 were measured using the wavelength dispersive spectroscopy (WDS) technique except for $x = 0.32$, whose composition was estimated from comparison with a T_c-x phase diagram in Ref. [41]. Four-probe measurements of in-plane resistivity were performed with a Quantum Design Physical Property Measurement System (PPMS). Samples for resistivity measurements had typical dimensions of (1–2) × 0.5 × (0.02–0.1) mm^3. Electrical contacts to samples prior to irradiation were made by soldering 50-μm silver wires with ultrapure tin solder, as described in Ref. [43]. The in-plane London penetration depth $\Delta\lambda(T)$ was measured using a self-oscillating tunnel-diode resonator technique [44,45]. The samples had typical dimensions of $0.5 \times 0.5 \times 0.03$ mm^3. Details of the measurements and calibration can be found elsewhere [44]. The 2.5 MeV electron irradiation was performed at the SIRIUS Pelletron facility of the Laboratoire des Solides Irradiés (LSI) at the École Polytechnique in Palaiseau, France [28]. The acquired irradiation dose is conveniently measured in C/cm^2, where $1\,\mathrm{C/cm^2} = 6.24 \times 10^{18}$ electrons/cm^2. The details of the measurements and doses of electron irradiation are summarized in Table I. London penetration depths in samples 0.26-B and 0.34-B were measured in the same samples before and after the irradiation. For these samples, resistivity after electron irradiation was measured by gluing the contacts with silver paint to prevent defect annealing during the soldering process. (This, of course, is not the optimal technique, but otherwise, the induced defects could be annealed by the soldering.) Samples 0.26-A and 0.26-B for resistivity were cut from the same large slab, and the same process was done for the 0.34-A and 0.34-B samples. For $x = 0.19$, the 0.19-A sample was prepared for resistivity measurements with soldered contacts. Its temperature-dependent resistivity was measured in pristine and irradiated states [see Fig. 1(a)]. Afterward, the contacts were removed to measure the London penetration depth.

TABLE I. List of samples measured before and after electron irradiation. $1\,\mathrm{C/cm^2} = 6.24 \times 10^{18}$ electrons/cm^2. WDS was conducted for the $x = 0.19$,0.26, and 0.34 samples. For the $x = 0.32$ sample, x was estimated by comparing its T_c with a T_c-x phase diagram in Ref. [41].

x	Sample label	Measurement
0.19	0.19-A	ρ before irradiation
	0.19-A	ρ after 1.8 C/cm^2 irradiation
	0.19-A	$\Delta\lambda$ after 1.8 C/cm^2 irradiation
	0.19-B	$\Delta\lambda$ before irradiation
0.26	0.26-A	ρ before irradiation
	0.26-B	$\Delta\lambda$ before irradiation
	0.26-B	$\Delta\lambda$ after 1.5 C/cm^2 irradiation
	0.26-B	ρ after 1.5 C/cm^2 irradiation
	0.26-B	$\Delta\lambda$ after 1.5 + 1.1 C/cm^2 irradiation
0.32	0.32-A	$\Delta\lambda$ before irradiation
	0.32-A	$\Delta\lambda$ after 8.3 C/cm^2 irradiation
0.34	0.34-A	ρ before irradiation
	0.34-B	$\Delta\lambda$ before irradiation
	0.34-B	$\Delta\lambda$ after 2.0 C/cm^2 irradiation
	0.34-B	ρ after 2.0 C/cm^2 irradiation

III. RESULTS AND DISCUSSION

Figure 1 shows normalized in-plane resistivity $\rho(T)/\rho(300\ \mathrm{K})$ measured before and after electron irradiation in samples with (a) $x = 0.19$, (b) $x = 0.26$, and (c) $x = 0.34$. Insets zoom in on superconducting transitions. For

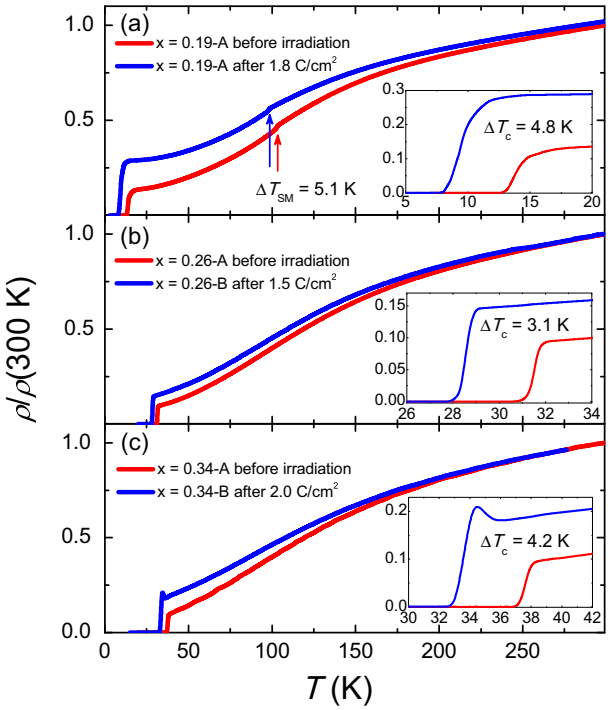

FIG. 1. (Color online) Evolution of the temperature-dependent resistivity (normalized by the value at 300K) with electron irradiation: (a) $x = 0.19$-A, (b) $x = 0.26$-A and 0.26-B, and (c) $x = 0.34$-A and 0.34-B. Insets zoom in on the superconducting transitions.

samples of all three doping levels, the introduction of disorder leads to a notable increase of the residual resistivity. The superconducting transition temperature T_c was determined by linear extrapolation of $\rho(T)$ at the transition to $\rho = 0$. Overall, the irradiation doses of 1.5 to 2.0 C/cm^2 lead to T_c decreasing by 3 to 5 K (see Fig. 4). Samples with $x = 0.26$ and $x = 0.34$ were outside the range of the coexisting magnetism and superconductivity. For $x = 0.19$, in addition to superconductivity, the long-range magnetic order develops simultaneously with orthorhombic distortion below the structural/magnetic transition T_{sm}. This transition is revealed as a small feature in $\rho(T)$, marked by the up arrows in Fig. 1(a). T_{sm} before irradiation was about 103 K, consistent with the previous report [46]. Irradiation with 1.8 C/cm^2 leads to T_{sm} decreasing by 5.1 K, supporting the itinerant nature of antiferromagnetism [47]. A "bump" in $\rho(T)$ above T_c developed after the irradiation in the sample with $x = 0.34$, similar to electron-irradiated $YBa_2Cu_3O_{7-\delta}$, where the bump was interpreted to be due to localization effects [29]. However, more likely this feature is an artifact of the measurements caused by high and temperature-dependent contact resistance. Sample 0.34-B was small since it was initially used for penetration depth measurement. To measure resistivity, the contacts were glued on later.

Figure 2 shows the variation of T_c/T_{c0} versus $\Delta\rho(T_c)$. From these values, we estimated the dimensionless scattering rate g^λ, defined in a simple form as [7,48]

$$g^\lambda = \frac{\hbar}{2\pi k_B \mu_0} \frac{\Delta\rho(T_c)}{T_{c0}\lambda(0)^2}, \quad (1)$$

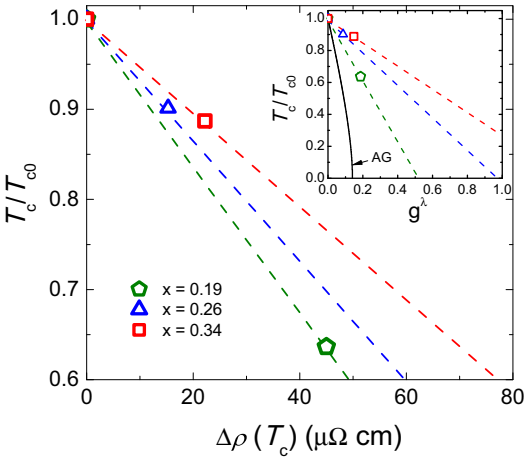

FIG. 2. (Color online) Evolution of T_c/T_{c0} as a function of $\Delta\rho(T_c)$ upon electron irradiation, where $\rho(T_c)$ is the resistivity right above T_c and $\Delta\rho(T_c)$ is the change of the resistivity after irradiation. The inset shows T_c/T_{c0} vs the dimensionless scattering rate g^λ. The classical Abrikosov-Gor'kov (AG) theory for an isotropic s-wave superconductor with magnetic impurities is also shown by a solid line [2].

where $\Delta\rho(T_c)$ is the change in resistivity at T_c after the irradiation. Zero-temperature London penetration depth $\lambda(0)$ was estimated from the Homes scaling [49], which takes into account both the doping dependence and the change with pair-breaking scattering [33] (see Fig. 7 and the corresponding discussion). The g^λ estimated from Eq. (1) is plotted in the inset of Fig. 2. The largest variation of $d(T_c/T_{c0})/dg^\lambda = -1.94$ was obtained for $x = 0.19$, while the smallest change of $d(T_c/T_{c0})/dg^\lambda = -0.76$ for $x = 0.34$. This indicates that the electron irradiation is more efficient for underdoped compounds, which have a fragile superconductivity competing with long-range magnetism.

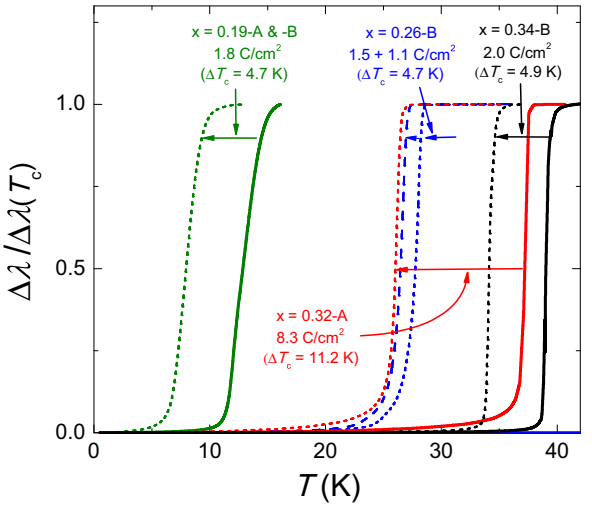

FIG. 3. (Color online) Variation of normalized in-plane penetration depth $\Delta\lambda(T)/\Delta\lambda(T_c)$ before and after electron irradiation; see Table I for the details on the samples.

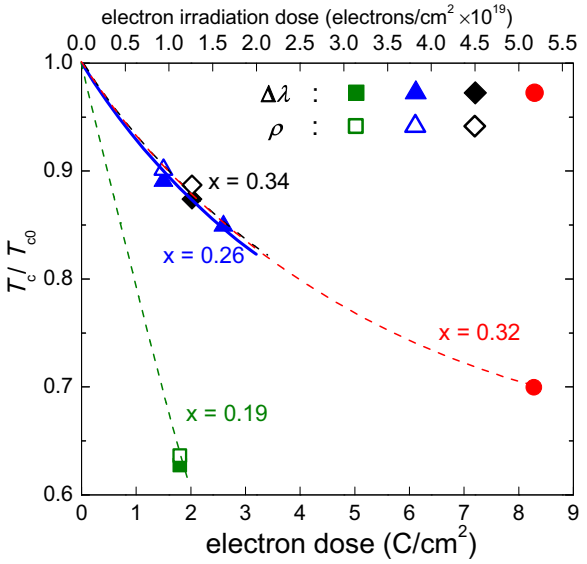

FIG. 4. (Color online) Variation of the reduced critical temperature T_c/T_{c0} with the dose of electron irradiation for samples with $x = 0.19$ (green squares), $x = 0.26$ (blue triangles), $x = 0.26$ (black diamonds), and $x = 0.34$ (red circles).

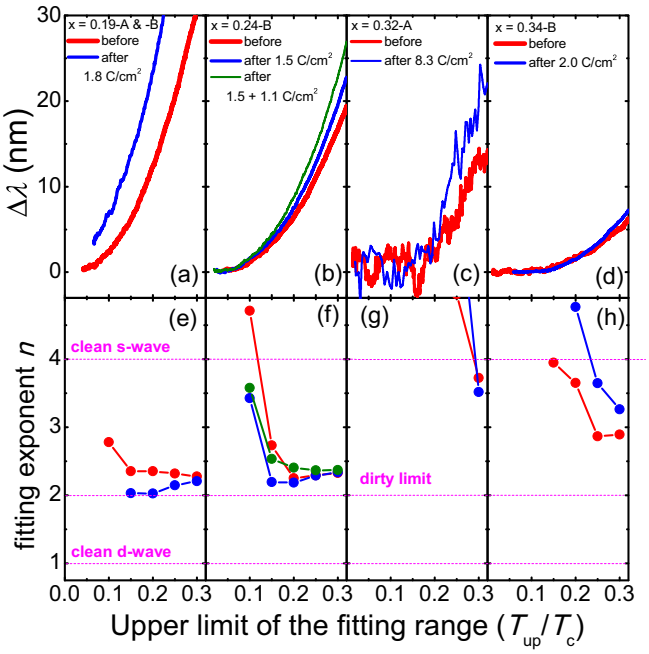

FIG. 5. (Color online) Low-temperature part of $\Delta\lambda(T)$ before and after electron irradiation of samples with (a) $x = 0.19$, (b) $x = 0.26$, (c) $x = 0.32$, and (d) $x = 0.34$. The data were analyzed with a power-law function, $\Delta\lambda = A(T/T_c)^n$, over a variable temperature range from the base temperature to a temperature T_{up}. (e)–(h) Corresponding fit exponents. The fitting errors are less than ± 0.1.

Figure 3 shows the normalized variation of the London penetration depth $\Delta\lambda(T)$ measured down to ~450 mK before and after electron irradiation for all three compositions. The magnetic superconducting transition temperature T_c was defined at a point of 50% change in $\Delta\lambda(T)$ at T_c and was consistent with the transport measurements shown in Fig. 1. The superconducting phase transition remained sharp even at the highest dose of 8.3 C/cm^2, which caused T_c to decrease by 11.2 K for the $x = 0.32$ sample. Figure 4 summarizes the reduced T_c/T_{c0} obtained from resistivity (open symbols) and penetration depth (solid symbols) data plotted versus electron-irradiation dose, where T_{c0} is the T_c before irradiation. The variations of T_c/T_{c0} for the $x = 0.26, 0.32$, and 0.34 samples were about $\Delta T_c/T_{c0} \simeq -0.04\,\mathrm{C}^{-1}\,\mathrm{cm}^{-2}$, whereas for the most underdoped sample with $x = 0.19$ we find a five times larger value of $\Delta T_c/T_{c0} \simeq -0.2\,\mathrm{C}^{-1}\,\mathrm{cm}^{-2}$. Qualitatively, the observed doping dependence of the effect of electron irradiation on T_c is similar to electron-doped $Ba(Fe_{1-x}Co_x)As_2$ [28].

To quantify the evolution of the superconducting gap structure, we analyzed the low-temperature part of $\Delta\lambda(T)$ as shown in Fig. 5. The absolute change $\Delta\lambda(T) = \lambda(0.3T/T_c) - \lambda(T_{min}/T_c)$ clearly increases after the irradiation, indicating enhanced pair breaking upon introduction of additional disorder. However, the low-temperature $\Delta\lambda(T)$ of the two nearly optimally doped samples, 0.32-A and 0.34-B, still clearly show exponential saturation below $0.2\ T/T_c$ even after the irradiation. This result suggests that the optimally doped compositions with isotropic superconducting gaps are extremely robust against electron irradiation, even at the very large dose of 8.3 C/cm^2, which caused suppression of T_c by 11.2 K, or $\Delta T_c \approx 0.3T_{c0}$. The situation is similar in a slightly underdoped sample at $x = 0.26$ in which the low-temperature saturation is seen below $0.1T/T_c$. In stark contrast, in the most underdoped sample with $x = 0.19$, where superconductivity and magnetism coexist, the saturating behavior disappears after the irradiation.

These observations become more apparent when the low-temperature $\Delta\lambda(T)$ is fitted using a power-law function, $\Delta\lambda = A(T/T_c)^n$. The results are plotted in Figs. 5(e)–5(h). To eliminate the uncertainty related to the upper fitting limit, we performed several fitting runs with a variable high-temperature end of the fitting range, T_{up}/T_c, from 0.1 to 0.3, while keeping the lower limit at the base temperature. The strong saturation behavior of the higher-doping samples is apparent from the large exponent values, $n > 3$, even for the very large irradiation dose of 8.3 C/cm^2. For the $x = 0.26$ sample, n increases as T_{up}/T_c decreases. This implies that the gap remains nodeless but develops anisotropy with a minimum value about two times smaller than in the cases of the $x = 0.32$ and 0.34 samples. For the most underdoped sample, $x = 0.19$, there is a clear evolution toward the dirty T^2 limit. In the pristine state, the exponent n varies from $n \approx 2.3$ at the widest range to 2.6–2.8 at the narrowest T_{up}/T_c range. However, after the irradiation, this tendency reverses. As T_{up}/T_c decreases, n starts to decrease toward $n = 2$. This is clearly shown in Fig. 6, where $\Delta\lambda$ is plotted vs $(T/T_c)^2$. While the data before the irradiation show an upward deviation from T^2, the postirradiated curve is a clean T^2 line.

Another way to analyze the data is to study the normalized superfluid density, $\rho_s(T) = \lambda^2(0)/\lambda^2(T)$. Figure 7 shows $\rho_s(T)$ before and after electron irradiation. Since the values of $\lambda(0)$ are not known, we first used the literature value of $\lambda(0) = 200$ nm found for unirradiated optimally doped

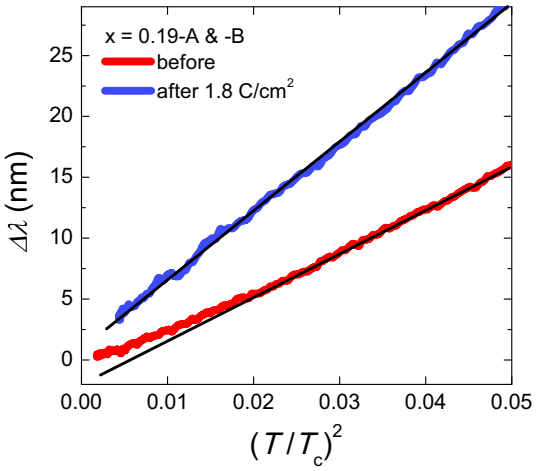

FIG. 6. (Color online) Low-temperature part of $\Delta\lambda$ of the sample with $x = 0.19$ before and after electron irradiation plotted as a function of $(T/T_c)^2$. The straight lines are the guides for the pure T^2 behavior.

samples, $x = 0.34$ [50–53]. Then, we used the Homes scaling, $\lambda^2(0) \propto \rho(T_c)/T_c$ [49]. Here $\rho(T_c)$ is the resistivity at T_c. The estimated values are $\lambda(0) = 226$ and 356 nm for the $x = 0.26$ ($T_c = 24.3$ K) and $x = 0.19$ ($T_c = 13.2$ K) samples, respectively. In addition, the maximum possible increase of $\lambda(0)$ induced by the irradiation was estimated by correlating the change of T_c with the pair-breaking scattering and relating it to the expected change of $\lambda(0)$ [33]. For example, for the $x = 0.32$-A sample, $\Delta T_c = -11.2$ K after 8.3 C/cm^2 irradiation, so the estimate of $\lambda(0)$ is about 238 nm. Following these two-step procedures, we estimated the doping and irradiation

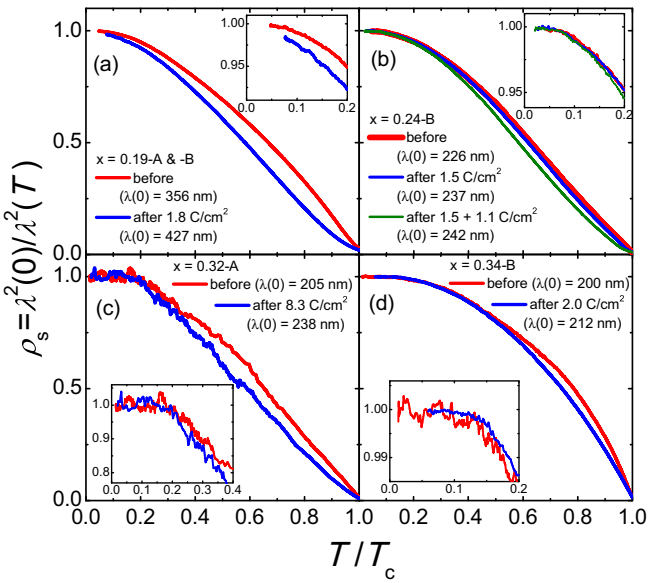

FIG. 7. (Color online) Normalized superfluid density, $\rho_s = [\lambda(0)/\lambda(T)]^2$, before and after electron irradiation for (a) $x = 0.19$, (b) $x = 0.26$, (c) $x = 0.32$, and (d) $x = 0.34$. Doping-dependent $\lambda(0)$ was estimated considering resistivity right above T_c (Homes scaling) and an irradiation-induced T_c decrease; see the text for details.

dependence of $\lambda(0)$. All values are shown in the legends in Fig. 7.

The superfluid density $\rho_s(T/T_c)$ is displayed in Fig. 7, and it is quite different for samples with different x. For a nearly optimally doped sample with $x = 0.34$ [Fig. 7(d)], the overall behavior follows the expectations for an s-wave-type pairing. Despite the change in T_c, the irradiation did not change the functional form of $\rho_s(T/T_c)$ much. As the composition moves toward the underdoped side (the $x = 0.32$ and 0.26 samples), the region of saturation shrinks but still exists at the lowest temperatures, below $0.2T/T_c$ ($x = 0.32$) and $0.1T/T_c$ ($x = 0.26$). This small saturation region remains almost intact upon high irradiation of 8.3 C/cm^2 ($x = 0.32$) and irradiation of 2.6 C/cm^2 ($x = 0.26$). In contrast, the superfluid density shows the largest change in the most underdoped sample, $x = 0.19$, where even minor signs of saturation in the preirradiated sample disappear after the irradiation. This suggests that the superconducting gap is very anisotropic in heavily underdoped samples and therefore is most susceptible to the defects induced by electron irradiation. This result is also consistent with the observation that the largest T_c suppression is found in the most underdoped sample (see Fig. 4). Overall, the full temperature-range shape of $\rho_s(T)$ is close to a full-gap s-wave behavior in the optimally doped sample and to a line-nodal curve for the most underdoped sample, $x = 0.19$.

IV. CONCLUSIONS

To summarize, the effects of electron irradiation on the in-plane resistivity and London penetration depth were studied in single crystals of the hole-doped $(Ba_{1-x}K_x)Fe_2As_2$ superconductor. The irradiation leads to the suppression of the superconducting T_c and of the temperature of the structural/magnetic transition T_{sm}. The suppression of T_c is much more rapid in the underdoped sample with $x = 0.19$, in which superconductivity coexists with the long-range magnetic order. This is consistent with the development of significant gap anisotropy in the coexisting phase. In the coexisting phase, the irradiation might even induce gapless superconductivity. Considering our previous study [36] and the prediction for the rate of suppression of T_c in the extended $s_\pm$ model [6], we suggest that the interband to intraband pairing ratio increases when moving away from the optimal concentration.

ACKNOWLEDGMENTS

We thank A. Chubukov, P. Hirschfeld, V. Mishra, and T. Shibauchi for useful discussions. This work was supported by the US Department of Energy (DOE), Office of Science, Basic Energy Sciences, Materials Science and Engineering Division. Ames Laboratory is operated for the US Department of Energy (DOE) (USA), by Iowa State University under Contract No. DE-AC02-07CH11358. We thank the SIRIUS team, B. Boizot, V. Metayer, and J. Losco, for running electron irradiation at Ecole Polytechnique (supported by the EMIR network, Proposal No. 11-11-0121.) Work in China was supported by the Ministry of Science and Technology of China, Project No. 2011CBA00102.

[1] P. W. Anderson, J. Phys. Chem. Solids **11**, 26 (1959).

[2] A. A. Abrikosov and L. P. Gor'kov, Zh. Eksp. Teor. Fiz. **39**, 1781 (1960) [Sov. Phys. JETP **12**, 1243 (1961)].

[3] P. J. Hirschfeld and N. Goldenfeld, Phys. Rev. B **48**, 4219 (1993).

[4] H. Kim, G. Preosti, and P. Muzikar, Phys. Rev. B **49**, 3544 (1994).

[5] A. V. Balatsky, I. Vekhter, and J.-X. Zhu, Rev. Mod. Phys. **78**, 373 (2006).

[6] Y. Wang, A. Kreisel, P. J. Hirschfeld, and V. Mishra, Phys. Rev. B **87**, 094504 (2013).

[7] R. Prozorov, M. Kończykowski, M. A. Tanatar, A. Thaler, S. L. Bud'ko, P. C. Canfield, V. Mishra, and P. J. Hirschfeld, arXiv:1405.3255.

[8] Y. Mizukami, M. Kończykowski, Y. Kawamoto, S. Kurata, S. Kasahara, K. Hashimoto, V. Mishra, A. Kreisel, Y. Wang, P. J. Hirschfeld, Y. Matsuda, and T. Shibauchi, arXiv:1405.6951.

[9] G. Xiao, M. Z. Cieplak, J. Q. Xiao, and C. L. Chien, Phys. Rev. B **42**, 8752 (1990).

[10] I. Mazin and J. Schmalian, Phys. C (Amsterdam, Neth.) **469**, 614 (2009).

[11] P. J. Hirschfeld, M. M. Korshunov, and I. I. Mazin, Rep. Prog. Phys. **74**, 124508 (2011).

[12] A. Chubukov, Annu. Rev. Condens. Matter Phys. **3**, 57 (2012).

[13] V. Mishra, G. Boyd, S. Graser, T. Maier, P. J. Hirschfeld, and D. J. Scalapino, Phys. Rev. B **79**, 094512 (2009).

[14] A. A. Golubov and I. I. Mazin, Phys. Rev. B **55**, 15146 (1997).

[15] T. Klein, R. Marlaud, C. Marcenat, H. Cercellier, M. Konczykowski, C. J. van der Beek, V. Mosser, H. S. Lee, and S. I. Lee, Phys. Rev. Lett. **105**, 047001 (2010).

[16] Y. Senga and H. Kontani, J. Phys. Soc. Jpn. **77**, 113710 (2008).

[17] S. Onari and H. Kontani, Phys. Rev. Lett. **103**, 177001 (2009).

[18] P. Cheng, B. Shen, J. Hu, and H.-H. Wen, Phys. Rev. B **81**, 174529 (2010).

[19] J. Li, Y. Guo, S. Zhang, S. Yu, Y. Tsujimoto, H. Kontani, K. Yamaura, and E. Takayama-Muromachi, Phys. Rev. B **84**, 020513 (2011).

[20] J. Li, Y. F. Guo, S. B. Zhang, J. Yuan, Y. Tsujimoto, X. Wang, C. I. Sathish, Y. Sun, S. Yu, W. Yi, K. Yamaura, E. Takayama-Muromachiu, Y. Shirako, M. Akaogi, and H. Kontani, Phys. Rev. B **85**, 214509 (2012).

[21] H. Kim, R. T. Gordon, M. A. Tanatar, J. Hua, U. Welp, W. K. Kwok, N. Ni, S. L. Bud'ko, P. C. Canfield, A. B. Vorontsov, and R. Prozorov, Phys. Rev. B **82**, 060518 (2010).

[22] C. Tarantini, M. Putti, A. Gurevich, Y. Shen, R. K. Singh, J. M. Rowell, N. Newman, D. C. Larbalestier, P. Cheng, Y. Jia, and H.-H. Wen, Phys. Rev. Lett. **104**, 087002 (2010).

[23] Y. Nakajima, T. Taen, Y. Tsuchiya, T. Tamegai, H. Kitamura, and T. Murakami, Phys. Rev. B **82**, 220504 (2010).

[24] J. Murphy, M. A. Tanatar, H. Kim, W. Kwok, U. Welp, D. Graf, J. S. Brooks, S. L. Bud'ko, P. C. Canfield, and R. Prozorov, Phys. Rev. B **88**, 054514 (2013).

[25] N. W. Salovich, H. Kim, A. K. Ghosh, R. W. Giannetta, W. Kwok, U. Welp, B. Shen, S. Zhu, H.-H. Wen, M. A. Tanatar, and R. Prozorov, Phys. Rev. B **87**, 180502 (2013).

[26] T. Taen, F. Ohtake, H. Akiyama, H. Inoue, Y. Sun, S. Pyon, T. Tamegai, and H. Kitamura, Phys. Rev. B **88**, 224514 (2013).

[27] A. C. Damask and G. J. Dienes, *Point Defects in Metals* (Gordon and Breach, New York, 1963).

[28] C. J. van der Beek, S. Demirdis, D. Colson, F. Rullier-Albenque, Y. Fasano, T. Shibauchi, Y. Matsuda, S. Kasahara, P. Gierlowski, and M. Konczykowski, J. Phys. Conf. Ser. **449**, 012023 (2013).

[29] F. Rullier-Albenque, H. Alloul, and R. Tourbot, Phys. Rev. Lett. **91**, 047001 (2003).

[30] M. Tinkham, *Introduction to Superconductivity*, 2nd ed., Dover Books on Physics (Dover, Mineola, NY, 2004).

[31] S. K. Yip and J. A. Sauls, Phys. Rev. Lett. **69**, 2264 (1992).

[32] D. Xu, S. K. Yip, and J. A. Sauls, Phys. Rev. B **51**, 16233 (1995).

[33] V. G. Kogan, R. Prozorov, and V. Mishra, Phys. Rev. B **88**, 224508 (2013).

[34] C. P. Strehlow, M. Kończykowski, J. A. Murphy, S. Teknowijoyo, K. Cho, M. A. Tanatar, T. Kobayashi, S. Miyasaka, S. Tajima, and R. Prozorov, Phys. Rev. B **90**, 020508 (2014).

[35] J.-Ph. Reid *et al.*, Supercond. Sci. Technol. **25**, 084013 (2012).

[36] H. Kim, M. A. Tanatar, W. E. Straszheim, K. Cho, J. Murphy, N. Spyrison, J.-Ph. Reid, B. Shen, H.-H. Wen, R. M. Fernandes, and R. Prozorov, Phys. Rev. B **90**, 014517 (2014).

[37] H. Fukazawa, Y. Yamada, K. Kondo, T. Saito, Y. Kohori, K. Kuga, Y. Matsumoto, S. Nakatsuji, H. Kito, P. M. Shirage, K. Kihou, N. Takeshita, C.-H. Lee, A. Iyo, and H. Eisaki, J. Phys. Soc. Jpn. **78**, 083712 (2009).

[38] K. Okazaki *et al.*, Science **337**, 1314 (2012).

[39] J.-Ph. Reid, M. A. Tanatar, A. Juneau-Fecteau, R. T. Gordon, S. R. de Cotret, N. Doiron-Leyraud, T. Saito, H. Fukazawa, Y. Kohori, K. Kihou, C. H. Lee, A. Iyo, H. Eisaki, R. Prozorov, and L. Taillefer, Phys. Rev. Lett. **109**, 087001 (2012).

[40] Z. Li, R. Zhou, Y. Liu, D. L. Sun, J. Yang, C. T. Lin, and G.-q. Zheng, Phys. Rev. B **86**, 180501 (2012).

[41] M. A. Tanatar, W. E. Straszheim, H. Kim, J. Murphy, N. Spyrison, E. C. Blomberg, K. Cho, J.-Ph. Reid, B. Shen, L. Taillefer, H.-H. Wen, and R. Prozorov, Phys. Rev. B **89**, 144514 (2014).

[42] H. Luo, Z. Wang, H. Yang, P. Cheng, X. Zhu, and H.-H. Wen, Supercond. Sci. Technol. **21**, 125014 (2008).

[43] M. A. Tanatar, N. Ni, S. L. Bud'ko, P. C. Canfield, and R. Prozorov, Supercond. Sci. Technol. **23**, 054002 (2010).

[44] R. Prozorov and R. W. Giannetta, Supercond. Sci. Technol. **19**, R41 (2006).

[45] R. Prozorov, R. W. Giannetta, A. Carrington, and F. M. Araujo-Moreira, Phys. Rev. B **62**, 115 (2000).

[46] B. Shen, H. Yang, Z.-S. Wang, F. Han, B. Zeng, L. Shan, C. Ren, and H.-H. Wen, Phys. Rev. B **84**, 184512 (2011).

[47] R. M. Fernandes, M. G. Vavilov, and A. V. Chubukov, Phys. Rev. B **85**, 140512 (2012).

[48] V. G. Kogan, Phys. Rev. B **80**, 214532 (2009).

[49] C. C. Homes, S. V. Dordevic, M. Strongin, D. A. Bonn, R. Liang, W. N. Hardy, S. Komiya, Y. Ando, G. Yu, N. Kaneko, X. Zhao, M. Greven, D. N. Basov, and T. Timusk, Nature (London) **430**, 539 (2004).

[50] C. Martin, R. T. Gordon, M. A. Tanatar, H. Kim, N. Ni, S. L. Bud'ko, P. C. Canfield, H. Luo, H. H. Wen, Z. Wang, A. B. Vorontsov, V. G. Kogan, and R. Prozorov, Phys. Rev. B **80**, 020501 (2009).

[51] C. Ren, Z.-S. Wang, H.-Q. Luo, H. Yang, L. Shan, and H.-H. Wen, Phys. Rev. Lett. **101**, 257006 (2008).

[52] G. Li, W. Z. Hu, J. Dong, Z. Li, P. Zheng, G. F. Chen, J. L. Luo, and N. L. Wang, Phys. Rev. Lett. **101**, 107004 (2008).

[53] D. V. Evtushinsky, D. S. Inosov, V. B. Zabolotnyy, M. S. Viazovska, R. Khasanov, A. Amato, H.-H. Klauss, H. Luetkens, C. Niedermayer, G. L. Sun, V. Hinkov, C. T. Lin, A. Varykhalov, A. Koitzsch, M. Knupfer, B. Buchner, A. A. Kordyuk, and S. V. Borisenko, New J. Phys. **11**, 055069 (2009).